24th COBEM - 2017

24th ABCM International Congress of Mechanical Engineering
December 3-8, 2017, Curitiba, PR, Brazil

COBEM-2017-0818
LATTICE BOLTZMANN SIMULATION OF A DROPLET INTERACTION WITH A SOLID SURFACE

Gustavo dos Santos Ribeiro
University of São Paulo, São Carlos School of Engineering, SP, Brazil
gustavo.santos.ribeiro@usp.br

Matheus dos Santos Guzella
Federal University of Jequitinhonha and Mucuri Valleys, Science and Tecnology Institute, MG, Brazil
matheus.guzella@ict.ufvjm.edu.br

Luben Cabezas-Gómez
University of São Paulo, São Carlos School of Engineering, SP, Brazil
lubencg@sc.usp.br

Abstract. *The Lattice Boltzmann (LB) method have been applied in the past years for the simulation of several thermo-fluid phenomena, including two-phase flow. In this paper is carried an analysis of the interaction of a droplet with a solid surface in a gas medium with a LB method, using a single component multiphase model of pseudopotentials. The results include the determination of the contact angle of droplets with the solid surface using Carnahan-Starling equation of state and different values of the artificial wall density.*

Keywords:*Lattice Boltzmann method, contact angle, droplet interaction, Shan-Chen model*

1. INTRODUCTION

The LB method is a mesoscopic procedure based on the kinetic theory of gases employing the Boltzmann transport equation (Chen *et al.*, 2014; Li *et al.*, 2016). The LB method has some advantages over traditional methods of CFD (Computational Fluid Dynamic), e.g.: the convective operator in the LB method is linear; and the boundary conditions are formulated by elementary mechanical arrangements by the interactions of molecules with solid walls. This work uses the method of pseudopotentials, initially proposed by Shan and Chen (Shan and Chen, 1993). In this method the fluid interactions are modeled by interparticle potential, whereby the separation of phases (gas and liquid) or components is automatically obtained without requiring any interphase capture technique (Sukop and Or, 2004).

2. COMPUTATIONAL PROCEDURE

2.1 Basic equations

The SC model was obtained from incorporating a body force to simulate attraction or repulsion interaction between the simulated particles. The discretized evolution equation for f, also called Lattice Boltzmann Equation (LBE), considering the most used approximation for the original collision integral, called BGK approximation, is given by (Huang *et al.*, 2015):

$$f_i(\mathbf{x}+\mathbf{c}_i\delta t, t+\delta t) - f_i(\mathbf{x},t) = -\frac{\delta t}{\tau}\left[f_i(\mathbf{x},t) - f_i^{eq}(\rho,\mathbf{u})\right] \tag{1}$$

In Eq. (1), $\mathbf{x}$ is the position vector, t is the time, $\mathbf{c}_i$ is the velocity vector set of the particles in the lattice structure, f_i is the discrete velocity distribution function, f_i^{eq} is the discrete equilibrium distribution function, δt is the time step, τ is the relaxation parameter and $\mathbf{u}$ is the macroscopic velocity vector field. A relation between the kinematic viscosity and the mesoscopic parameters can be obtained from Chapman-Enskog expansion (Guo and Shu, 2013):

$$\nu = c_s^2(\tau - \frac{1}{2}\delta t) \tag{2}$$

where c_s is the speed of the sound for the fluid. In this paper it is applied the discrete velocity model D3Q19, which allows 3D simulations, resulting $c_s = 1/\sqrt{3}$ (Huang *et al.*, 2015). Figure 1 presents the above mentioned discrete velocity model:

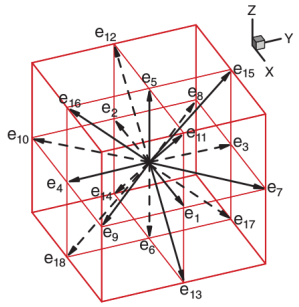

Figure 1: Lattice configuration for the D3Q19 discrete velocity model (Huang *et al.*, 2015)

The discrete equilibrium distribution function is written as (Huang *et al.*, 2015):

$$f_i^{eq}(\mathbf{x},t) = \rho w_i \left[1 + \frac{\mathbf{c}_i \cdot \mathbf{u}}{c_s^2} + \frac{(\mathbf{c}_i \cdot \mathbf{u})^2}{2c_s^4} - \frac{(\mathbf{u})^2}{2c_s^2}\right] \tag{3}$$

where w_i are the weighting parameters associated with the discrete velocity model (Guo and Shu, 2013):

$$w_i = \begin{cases} 1/3, & \text{for} \quad i = (0) \\ 1/18, & \text{for} \quad i = (1,\ldots,6) \\ 1/36, & \text{for} \quad i = (7,\ldots,18) \end{cases} \tag{4}$$

The discrete velocitiy set $\mathbf{c}_i$ for the D3Q19 lattice structure is given by (Guo and Shu, 2013):

$$[\mathbf{c}_0, \mathbf{c}_1, \ldots, \mathbf{c}_{18}] = c \begin{bmatrix} 0 & 1 & -1 & 0 & 0 & 0 & 1 & -1 & 1 & -1 & 1 & -1 & 1 & -1 & 0 & 0 & 0 & 0 \\ 0 & 0 & 0 & 1 & -1 & 0 & 1 & 1 & -1 & -1 & 0 & 0 & 0 & 0 & 1 & -1 & 1 & -1 \\ 0 & 0 & 0 & 0 & 0 & 1 & 0 & 0 & 0 & 0 & 1 & 1 & -1 & -1 & 1 & 1 & -1 & -1 \end{bmatrix} \tag{5}$$

where $c = \delta x/\delta t$ is the particle velocity. The macroscopic properties, such as fluid density and linear momentum, can be obtained from moments of the distribution function, such as:

$$\begin{aligned} \rho &= \sum_i f_i \\ \rho\mathbf{u} &= \sum_i f_i \mathbf{c}_i \end{aligned} \tag{6}$$

The inclusion of force terms in the traditional LBE can be acomplished by several different approaches (Krüger *et al.*, 2017). In a general form, the second-order time and space discretized LBE with a force source term can be expressed by:

$$f_i(\mathbf{x} + \mathbf{c}_i\delta t, t + \delta t) - f_i(\mathbf{x}, t) = \Omega_i(\mathbf{x}, t)\delta t + S_i(\mathbf{x}, t)\delta t \tag{7}$$

where Ω_i represents the discrete collision term, and S_i is the discrete force source term.

When a force term is included in the LBE, the velocity field must be redefined to guarantee the same time and space discretization accuracy as used to discretize the LBE with a force term (Krüger *et al.*, 2017). Also, in the original work of Shan and Chen (1993), the redefinition of the velocity can capture the change in the linear momentum due to the presence of a force field. The redefinition of the fluid velocity field is expressed by:

$$\mathbf{u} = \frac{1}{\rho}\sum_i \mathbf{c}_i f_i + \frac{\mathbf{F}\delta t}{2\rho} \tag{8}$$

where $\mathbf{F}$ represents the force term, in its general form expressed by:

$$\mathbf{F} = \mathbf{F}_{int}(\mathbf{x}) + \mathbf{F}_{ads}(\mathbf{x}) + \mathbf{F}_{g}(\mathbf{x}) \tag{9}$$

In Eq. (9), $\mathbf{F}_{int}$ represents the interparticle interaction force, which is responsible for the phase separation, $\mathbf{F}_{ads}$ represents the adhesion force between the fluid and solid surfaces, which is responsible for wettability, and $\mathbf{F}_{g}$ is the gravitational body force, neglected in the present work. The discretized interparticle interaction force term used in this work is given by the Eq. (10), represented through a sum of pseudopotential interactions with nearest lattice neighbours:

$$\mathbf{F}_{int}(\mathbf{x}, t) = -G\psi(\mathbf{x}, t) \sum_{i} w_i \psi(\mathbf{x} + \mathbf{c}_i \delta t, t)\mathbf{c}_i \tag{10}$$

where G represents the strength of the interaction (attractive or repulsive), ψ an effective density function which replaces the local density ρ, also called pseudopotential function (Krüger *et al.*, 2017).

The adhesion force between the gas/liquid phase and solid walls is calculated by Eq. (11):

$$\mathbf{F}_{ads}(\mathbf{x}, t) = -G\psi(\mathbf{x}, t) \sum_{i} w_i \psi(\rho_w) s(\mathbf{x} + \mathbf{c}_i \delta t, t)\mathbf{c}_i \tag{11}$$

The parameter ρ_w represents a fictitious solid phase density, and it is used to tune different wall wettability properties through changing the inter-particle potential at the wall $\psi(\rho_w)$. For example, if G is fixed at a constant value, setting $\rho_w = \rho_{liquid}$ leads to a contact angle of $\theta = 0°$, representing a full wetting condition. Moreover setting $\rho_w = \rho_{gas}$ results in $\theta = 180°$, which represents a completely hydrophobic surface. All other possible contact angle values can be realized by taking a value spanned between these two extremes (Benzi *et al.*, 2006; Chen *et al.*, 2014).

A widely accepted and often used form of the effective density function is (Krüger *et al.*, 2017):

$$\psi(\rho) = \rho_0 \left[1 - exp(\frac{-\rho}{\rho_0}) \right] \tag{12}$$

with a reference density ρ_0 that in simulation units is mostly se to unity. Through a Taylor series expansion, it is possible to show that $\psi(\rho) \approx \rho$ for $\rho << \rho_0$, when the pseudopotential reduces to the fluid density itself.

For the SC multiphase single component model, it is known that the equation of state (EOS) found by considering a force term, is expressed by (Huang *et al.*, 2015):

$$p = c_s^2 \rho + \frac{c_s^2 G}{2} \psi^2(\rho) \tag{13}$$

which indicates that the thermodynamic pressure p is a function of ψ. Alternatively, if the expression for a different EOS is known, it is possible to employ the Eq. (13) to provide the following definition of ψ (He and Doolen, 2002):

$$\psi = \sqrt{\frac{2(p - c_s^2 \rho)}{c_s^2 G}} \tag{14}$$

to replace Eq. (12).

Among the possibilities available for the choice of non-ideal EOS, the C-S EOS, obtained by Carnahan and Starling (1969), represents a more accurate expression for hard sphere systems and allows the simulation to achieve the highest density ratios for ρ_{liquid}/ρ_{gas}, and it is very well suited for application in LB method (Yuan and Schaefer, 2006). The C-S EOS is given by:

$$p = \rho RT \frac{1 + b\rho/4 + (b\rho/4)^2 - (b\rho/4)^3}{(1 - b\rho/4)^3} - a\rho^2 \tag{15}$$

whith $a = 0.4963 R^2 T_c^2 / p_c$ and $b = 0.18727 RT_c / p_c$, where T_c and p_c are the critical temperature and pressure, respectively.

2.2 Parameters selection

In LB method, the simulation are mostly performed in lattice units, a simple artificial set of dimensionless units scaled such that $\delta x = \delta t = 1$. Therefore, to relate the obtained results to real physical values, a correct choice of conversion factors must be ensured. Usually, parameter conversion can be performed through non-dimensional numbers, such as Reynolds number, which is often considered in single-component flows simulations. For multiphase flows however, depending on the simulation, a broader set of parameters is needed.

In this paper, we use the nondimensionalization of principal thermodynamical properties of interest through the concept of corresponding states, which states that the reduced properties should be the same no matter what kind of units are used. The reduced density, pressure and temperature are given, respectively, by:

$$\rho_r = \frac{\rho}{\rho_c}, \qquad p_r = \frac{p}{p_c}, \qquad T_r = \frac{T}{T_c} \tag{16}$$

where the subscripts "r" and "c" denote the reduced and critical properties. Therefore, a conversion can be achieved from a lattice property to a real property, *e.g.* $\rho^{phys} = \rho^{Lu}\rho_c^{phys}/\rho_c^{Lu}$, where the superscripts "$phys$" and "Lu" denote physical units and lattice unites, respectively.

The SC multiphase model is a diffuse-interface method, so the interface thickness is an important factor in simulations. A more stable simulation is achieved when the interface is thicker, but it returns results farther from reality. The interface thickness is not directly adjustable in SC multiphase model, which makes it dependent not only on the temperature or τ, but also the particular EOS chosen. In our case, the selection of the parameters a, b and R in the C-S EOS affects the interface thickness and numerical stability. Yuan and Schaefer (2006) setted $a = 1$, $b = 4$ and $R = 1$, in lattice units, for their study on C-S EOS. Huang *et al.* (2011) studied the effect of parameter variation, showing that this choice is appropriate because the interface thickness maintains approximately $5\delta x$, for most T and τ.

This paper presents a simulation of the static contact angle obtained for liquid droplets in vapor. Therefore, the domain is initialized considering the presence of a two-phase fluid in contact with a solid boundary. As discussed before, the main parameter to impose a wettability condition in the SC multiphase model is the parameter ρ_w. The system is initialized with a semi-spherical cap at the wall, and the initial densities difference follows the values predicted by the EOS, using the Maxwell construction, known as equal area rule, as explained below.

2.3 The Maxwell equal-area construction

In thermodynamics, the densities of a two-phase system is determined by the system equilibrium. The Maxwell construction is adopted to obtain the vapor and liquid densities from a given $p - v$ curve obtained from a specific EOS at a temperature below the critical point. The basic idea is that the areas of two regions above and below the saturation pressure should be equal, or:

$$\int_{v_l}^{v_v} p dv = p_0(v_v - v_l) \tag{17}$$

where p_0 is the saturation pressure at a given temperature.

Figure 2 shows the result obtained from a numerical procedure implemented to construct the C-S EOS, for $T_r = 0.8$ and the parameters (a, b, c) discussed before. For this case, the specific volume for the liquid and gas phases are $v_l = 3.257$ and $v_g = 48.554$ in lattice units respectively, which gives the initial densities $\rho_l = 0.31$ and $\rho_g = 0.021$. This numerical procedure can be used for different T_r values and is based on an optimization procedure to found the minimum difference between the two areas. Note that the T and P values are in lattice units.

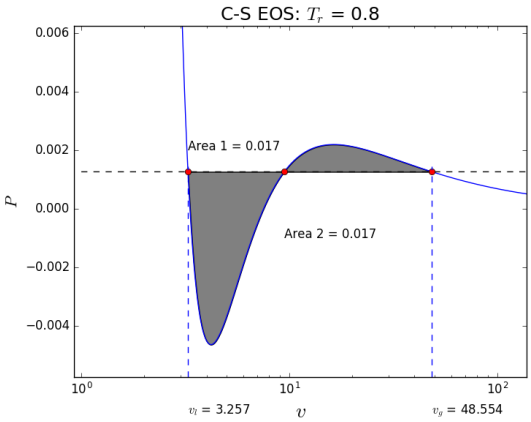

Figure 2: Implementation of the $p - v$ curve, in a semilog scale, for C-S EOS at $T = 0.8T_c$, $a = 1$, $b = 4$ and $R = 1$. All values are given in lattice units and were obtained using the Maxwell construction rule.

3. RESULTS

The computational domain in the simulation is composed of $l_x = 50\delta x$, $l_y = 50\delta x$ and $l_z = 40\delta x$, giving a total number of 51x51x41 nodes in each direction. The initial droplet have a radius of $r = 15\delta x$. The input parameters for the C-S EOS are $a = 1$, $b = 4$, $R = 1$ and $T_r = 0.8$, giving liquid and gas phase densities of $\rho_l = 0.31$ and $\rho_g = 0.021$, respectively, therefore the density ratio is about 15. In order to obtain different contact angles, the wettability parameter ρ_w received values ranging $\rho_g < \rho_w < \rho_l$. The obtained contact angles were measured using a graphical tool.

Figure 3 shows the result obtained for $\rho_w = 0.053$, corresponding to a case of an hydrophobic surface. Note that the contact angle for this case is high. equal to $\theta = 120°$, meaning that the wettability is low.

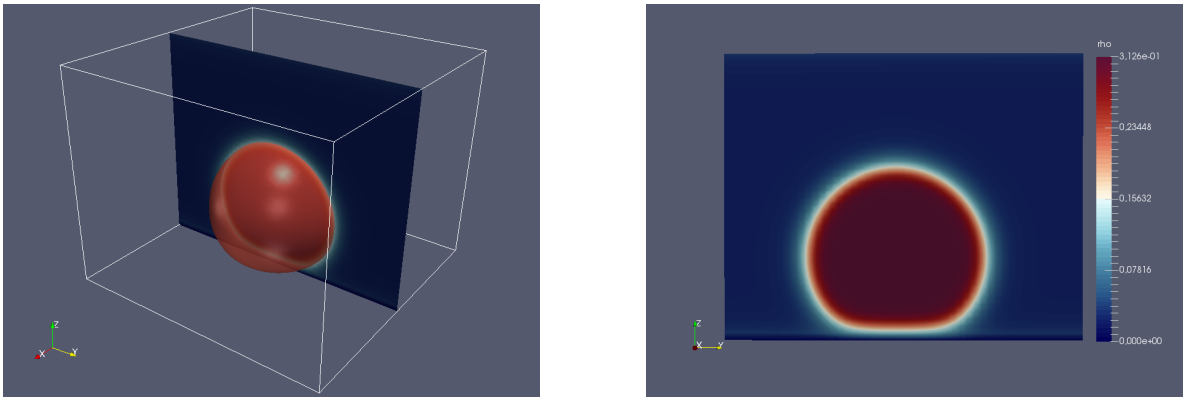

(a) (b)

Figure 3: $\rho_w = 0.053$, resulting in a contact angle of $\theta = 120°$: a) density contour, b) frontal section

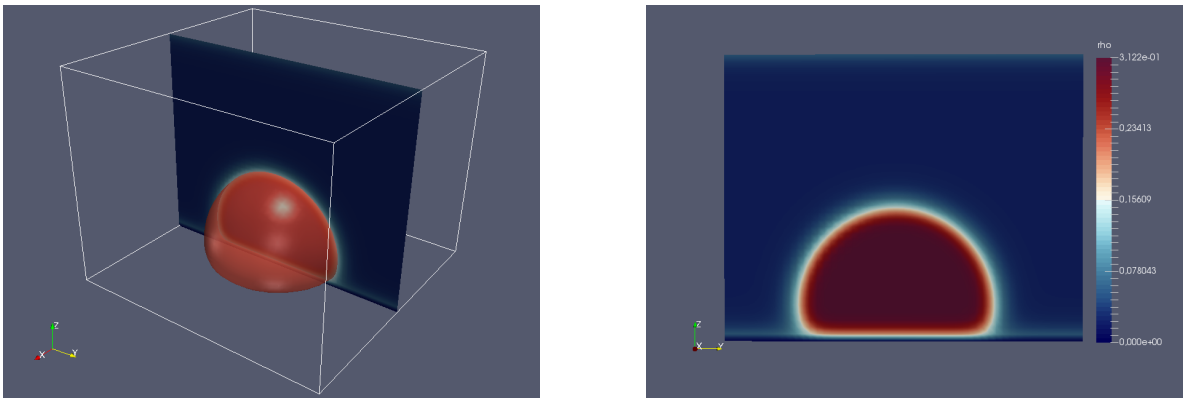

(a) (b)

Figure 4: $\rho_w = 0.100$, resulting in a contact angle of $\theta = 97°$: a) density contour, b) frontal section

An intermediary case between hydrophobic and hydrophilic surfaces is shown in Fig. 4. This results is obtained increasing the value or ρ_w. In this case $\rho_w = 0.100$, resulting in a contact angle of $\theta = 97°$.

A result for an hydrophilic surface is shown in Fig. 5. In this case $\rho_w = 0.190$, with a contact angle equal to $\theta = 39°$. An hydrophilic surface means that the wettability is high and the contact angle is small, leading a high adhesiveness between the fluid and solid surface. It should be noted that it is used a periodic boundary condition in all domain walls. This type of boundary conditions leads to a droplet division between bottom and upper numerical (domain) surfaces for a high values of ρ_w. This behavior is not shown in the commented figures, but was obtained in other simulation results.

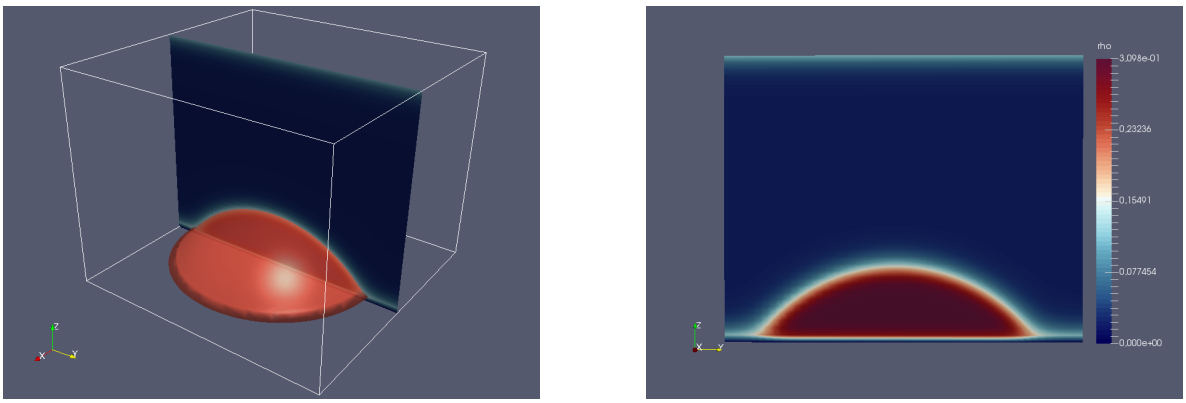

(a) (b)

Figure 5: $\rho_w = 0.190$, resulting in a contact angle of $\theta = 39°$: a) density contour, b) frontal section

In a second case, two smaller fluid droplets were inserted into the vapor domain, considering the same values for the C-S parameters as those used in the previous case. The distance between droplets has been adjusted so that they are close enough for a possible coalescence occurs. The results obtained are shown in Fig. 6, according to the time progress. As can be seen the two droplets collide, occurring their coalescence and a posterior attraction by the bottom domain surface (solid wall). Initially, the droplets feels a higher attraction force between it, leading to their collision and coalescence. After this phenomenon they collide with the bottom wall, leading to its interaction with it. This interaction represents an hydrophilic surface. It should be commented that the gravity force is not considered in the present simulations. It seems that the resultant droplet loses mass, but this behavior is under investigation and seems to be related to the used boundary conditions in the three-dimensional domain.

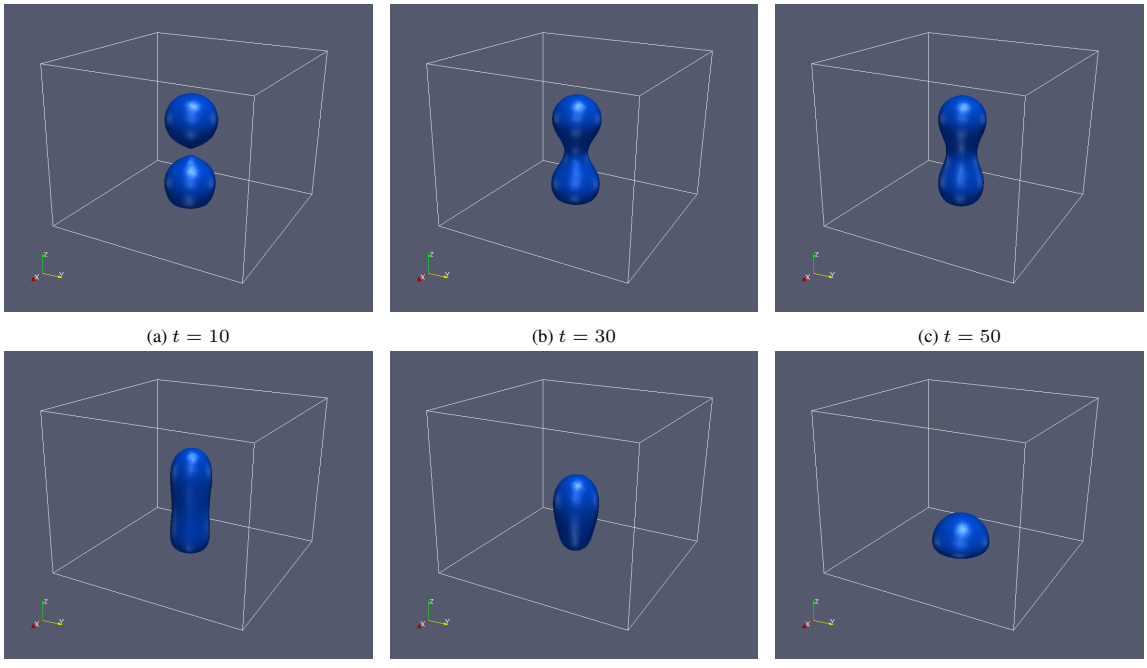

(a) $t = 10$ (b) $t = 30$ (c) $t = 50$

(d) $t = 100$ (e) $t = 200$ (f) $t = 400$

Figure 6: Three-dimensional simulation of two coalescing droplets, considering the wettability parameter $\rho_w = 0.1$

The same numerical simulation was performed in a two-dimensional domain. The results obtained in this case show that the liquid mass is conserved. This behavior can be observed in Fig. 7. In any case it is necessary to study further this

problem. Comparing these results with those obtained for a single droplet it can be said that the final contact angle will be the same.

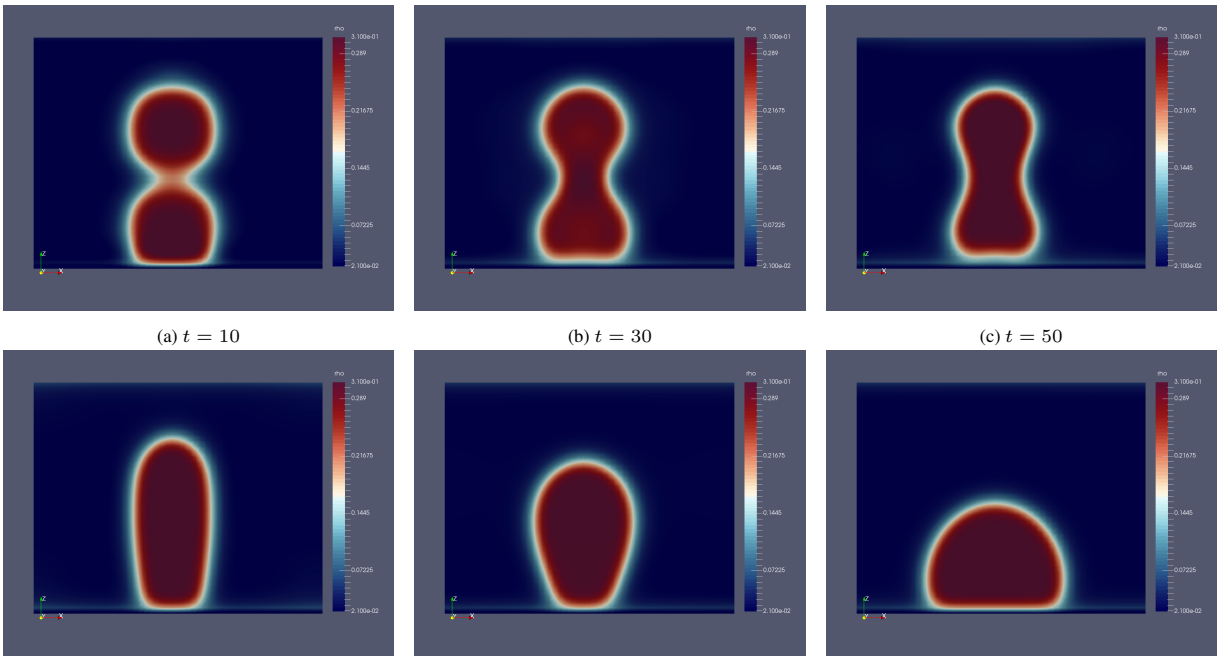

(a) $t = 10$ (b) $t = 30$ (c) $t = 50$

(d) $t = 100$ (e) $t = 200$ (f) $t = 400$

Figure 7: Two-dimensional simulation of two coalescing droplets, considering the wettability parameter $\rho_w = 0.1$

In Fig. 7 the last frame was obtained for 400 time steps. The droplet profile for this time steps has a contact angle almost equal to that obtained for a single droplet at the stationary state. Plotting the a snapshot for 2000 time steps in the case of composed droplet it is obtained the same contact angle for a single droplet. This behavior is shown in Fig. 8. This is an expected behavior because these two cases were simulated for $\rho_w = 0.100$.

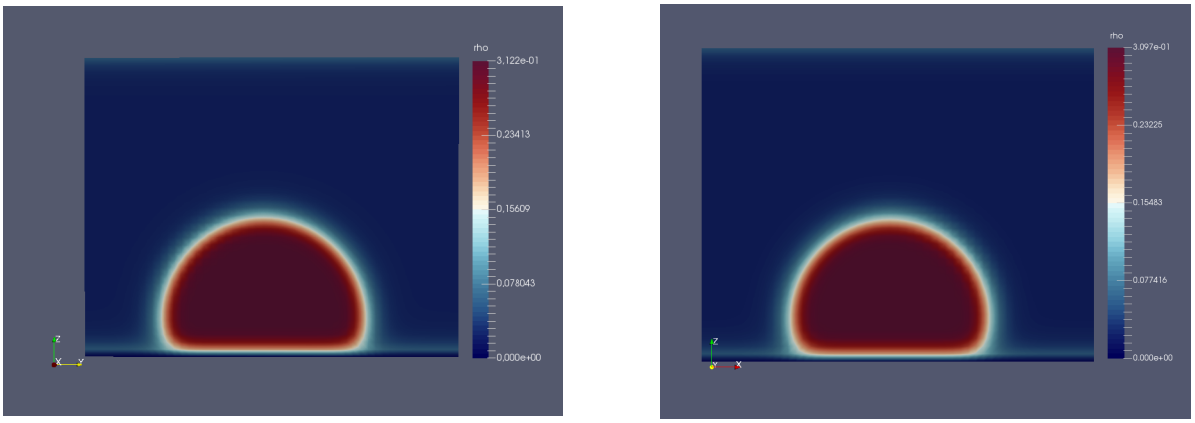

(a) (b)

Figure 8: Comparison of two cases showing the influence of the same wettability parameter $\rho_w = 0.100$: a) Three-dimensional simulation of a single droplet interaction with a solid boundary, with initial radius of $15\delta x$; b) Two-dimensional simulation of two droplets after coalescence, following a solid boundary interaction, with initial radius of $8\delta x$ each, for $t = 2000\delta t$.

4. CONCLUSION

The main conclusions that can be written from the obtained results are:

- The numerical implementation of the LB method is simple. The method easily allows the inclusion and analysis of the various forces that take place in the present problem;
- The S-C multiphase LB methodology is based on the application of thermodynamic concepts, helping to understand

physically the involved transport phenomena. In this respect, the method heavily depends on the right use of these concepts;

- The obtained numerical results are physically correct and show how different parameters influence the wettability parameter;
- It is important to observe the correct conversion from the physical units into the lattice units and vice-versa.

5. ACKNOWLEDGEMENTS

The authors fully acknowledge the financial support received from CNPq (process number 142283/2015-0) and FAPESP (process number 16/09509-1).

6. REFERENCES

Benzi, R., Biferale, L., Sbragaglia, M., Succi, S. and Toschi, F., 2006. "Mesoscopic modeling of a two-phase flow in the presence of boundaries: The contact angle". *Physical Review E*, Vol. 74, No. 2.

Carnahan, N.F. and Starling, K.E., 1969. "Equation of state for nonattracting rigid spheres". *Journal of Chemical Physics*, Vol. 51, No. 2, pp. 635–636.

Chen, L., Kang, Q., Mu, Y., He, Y. and Tao, W., 2014. "A critical review of the pseudopotential multiphase lattice boltzmann model: Methods and applications". *International Journal of Heat and Mass Transfer*, Vol. 76, pp. 210 – 236.

Guo, Z. and Shu, C., 2013. *Lattice Boltzmann Method and its Applications in Engineering*, Vol. 3 of *Advances in computational fluid dynamics*. World Scientific, Singapore.

He, X. and Doolen, G.D., 2002. "Thermodynamic foundations of kinetic theory and lattice boltzmann models for multiphase flows". *Journal of Statistical Physics*, Vol. 107, No. 112.

Huang, H., Krafczyk, M. and Lu, X., 2011. "Forcing term in single-phase and shan-chen-type multiphase lattice boltzmann models". *Physical Review E*, Vol. 84, No. 4.

Huang, H., Sukop, M. and Lu, X.Y., 2015. *Multiphase Lattice Boltzmann Methods: Theory and Application*. Wiley-Blackwell.

Krüger, T., Kusumaatmaja, H., Kuzmin, A., Shardt, O., Silva, G. and Viggen, E.M., 2017. *The Lattice Boltzmann Method*. Graduate texts in physics. Springer, Switzerland.

Li, Q., Luo, K.H., Kang, Q.J., He, Y.L., Chen, Q. and Liu, Q., 2016. "Lattice boltzmann methods for multiphase flow and phase-change heat transfer". *Progress in Energy and Combustion Science*, Vol. 52, pp. 62–105.

Shan, W. and Chen, H., 1993. "Lattice boltmzann model for simulating flows with multiple phases and components". *Physical Review E*, Vol. 47, No. 3, pp. 1815 – 1820.

Sukop, M.C. and Or, D., 2004. "Lattice boltzmann method for modeling liquid-vapor interface configurations in porous media". *Water Resources Research*, Vol. 40, No. 1.

Yuan, P. and Schaefer, L., 2006. "Equations of state in a lattice boltzmann model". *Physics of Fluids*, Vol. 18, No. 4, p. 042101.

7. RESPONSIBILITY NOTICE

The authors are the only responsible for the printed material included in this paper.